

# Effects of pre-irradiation annealing at high temperature on optical absorption and electron paramagnetic resonance of natural pumpellyite mineral



Henry Javier-Ccallata <sup>a,b,\*</sup>, Luiz Tomaz Filho <sup>c,d</sup>, Maria L. Sartorelli <sup>b</sup>, Shigueso Watanabe <sup>c</sup>

<sup>a</sup> Escuela de Ingeniería Electrónica y Telecomunicaciones, Universidad Alas Peruanas Filial Arequipa, Urb. D. A. Carrión G-14, J. L. Bustamante y Rivero, Arequipa, Peru

<sup>b</sup> Laboratório de Sistemas Nanoestruturados, Departamento de Física, Universidade Federal de Santa Catarina, Florianópolis, Santa Catarina, Brazil

<sup>c</sup> Departamento de Física Nuclear, Instituto de Física, Universidade de São Paulo, Rua do Matão, travessa R, 187, CEP 05508-900 São Paulo, SP, Brazil

<sup>d</sup> Faculdade de Tecnologia e Ciências Exatas, Universidade São Judas Tadeu, Rua Taquari 546, São Paulo, SP, Brazil

## ARTICLE INFO

### Article history:

Received 24 September 2012

Received in revised form 10 June 2013

Available online 8 July 2013

### Keywords:

Pumpellyite  
Optical absorption  
Annealing  
EPR  
Crystal field

## ABSTRACT

Natural silicate mineral of pumpellyite,  $\text{Ca}_2\text{MgAl}_2(\text{SiO}_4)(\text{Si}_2\text{O}_7)(\text{OH})_2(\text{H}_2\text{O})$ , point group A2/m, has been studied concerning high temperature annealing and  $\gamma$ -radiation effects on Optical Absorption (OA) and Electron Paramagnetic Resonance (EPR) properties. Chemical analysis revealed that besides Si, Al, Ca and Mg, other oxides i.e., Fe, Mn, Na, K, Ti and P are present in the structure as impurities. OA measurements of natural and annealed pumpellyite revealed several bands in the visible region due to spin forbidden transitions of  $\text{Fe}^{2+}$  and  $\text{Fe}^{3+}$ . The behaviour of bands around 900 and 1060 nm, with pre-annealing and  $\gamma$  radiation dose, indicating a transition  $\text{Fe}^{2+} \rightarrow \text{e}^- + \text{Fe}^{3+}$ . On the other hand, EPR measurements reveal six lines of  $\text{Mn}^{2+}$ , and satellites due to hyperfine interaction, superimposed on the signal of  $\text{Fe}^{3+}$  around of  $g = 2$ . For heat treatment from 800 °C the signal grows significantly and for 900 °C a strong signal of  $\text{Fe}^{3+}$  hides all  $\text{Mn}^{2+}$  lines. The strong growth of this signal indicates that the transitions are due to  $\text{Fe}^{3+}$  dipole–dipole interactions.

© 2013 Elsevier B.V. All rights reserved.

## 1. Introduction

To the epidote group belong following silicate minerals: epidote, zoisite, clinzozoisite, piemontite, allanite (ortite), lawsonite and pumpellyite [1]. All members of this group are characterized by having structures consisting of chains of edge-sharing ( $\text{SiO}_4$ ) tetrahedra parallel to y-axis and linked in the direction of z-axis by groups of single ( $\text{SiO}_4$ ) tetrahedra and of the double tetrahedra ( $\text{Si}_2\text{O}_7$ ). These chains produce relatively large cavities that can be occupied by large cations usually Ca, in nine or ten-fold coordination.

The composition formula of this group can be written:

$\text{X}_2\text{Y}_3\text{Z}_3(\text{O},\text{OH},\text{F})_{13}$   
in which: X = Ca, Ce, La, Y, Th,  $\text{Fe}^{2+}$ ,  $\text{Mn}^{2+}$ ,  $\text{Mn}^{3+}$ ;  
Y = Al,  $\text{Fe}^{3+}$ ,  $\text{Mn}^{3+}$ ,  $\text{Mn}^{2+}$ ,  $\text{Fe}^{2+}$ , Ti;  
Z = Si, Be

Dollase [2] shows the structure of clinzozoisite, which is common to other members of the epidote group. This means that besides that was described above we should add chains of

edge-sharing octahedrons of two kinds parallel to y-axis: the first consist of edge-sharing octahedra (M2), the second one is a chain two octahedra M1 and M3 attached on alternative sides along its length. While M2 contains only aluminum, M1 contains ions of Al, Mg and Fe. The M3 octahedra contain non-Al atoms, in most of cases  $\text{Fe}^{3+}$  and  $\text{Mn}^{2+}$ .

Tsang and Ghose [3] investigated the local environments of transition metal ions and their distributions among various aluminum and calcium sites in a gem quality tanzanite using Electron Paramagnetic Resonance (EPR) and Optical Absorption (OA) spectra. The metal ions in this case refer to  $\text{Mn}^{2+}$ ,  $\text{Fe}^{3+}$  and two types of  $\text{V}^{2+}$ . Srinivasulu et al. [4] investigated thulite, a manganese rich zoisite containing also Fe and found that the optical spectrum is mainly due to  $\text{Mn}^{2+}$  ions. The EPR measurements confirmed the presence of  $\text{Mn}^{2+}$  and  $\text{Fe}^{3+}$  ions. Taran and Langer [5] analyzed electronic absorption spectra of  $\text{Fe}^{3+}$  in andradite (garnet) and epidote at different temperatures (300–750 K) and pressures (up to 10 GPa). Nagashima et al. [6] investigated the distribution of Fe among octahedral sites and its effect on the crystal structure of pumpellyite collected from two places in Shimane Peninsula, Japan. For example the effect of  $\text{Fe}^{3+} \rightarrow \text{Al}^{3+}$  substitution at the Y site consist in increasing Y–O distances and values of the  $\text{YO}_6$  octahedra, where Y is given in the general formula of pumpellyite  $\text{W}_8\text{X}_4\text{Y}_8\text{Z}_{12}\text{O}_{56-n}(\text{OH})_n$ . Additionally, Nagashima et al. [6] have

\* Corresponding author at: Laboratório de Sistemas Nanoestruturados, Departamento de Física, Universidade Federal de Santa Catarina, Florianópolis, Santa Catarina, Brazil. Tel.: +51 973699188.

E-mail address: [henrysjc@gmail.com](mailto:henrysjc@gmail.com) (H. Javier-Ccallata).

shown that divalent and trivalent cations such as  $Mg^{2+}$ ,  $Al^{2+}$ ,  $Mn^{2+}$ ,  $Mn^{3+}$ ,  $Fe^{2+}$  and  $Fe^{3+}$  can occupy X site. The W site is subdivided into W1 and W2. The pumpellyite structure displays five-membered rings formed by corner-sharing disilicate, orthosilicate, X, and Y octahedra. Half of the rings are open and have W1 at their center, the others are closed and encase W2 [1]. The W1 and W2 sites are predominantly occupied by Ca.

Both X and Y are octahedrally coordinated but the  $[XO_6]$  octahedron is larger than the  $[YO_6]$  one. Both divalent and trivalent cations, such as  $Mg^{2+}$ ,  $Al^{3+}$ ,  $Mn^{2+}$ ,  $Mn^{3+}$ ,  $Fe^{2+}$ ,  $Fe^{3+}$ ,  $V^{3+}$  and  $Cr^{3+}$ , occupy X, whereas Y is occupied by trivalent cations only.

Nagashima et al. [7] studied the hydrogen bonds system in two samples of pumpellyite, one from Switzerland and other from Russia using electron-microprobe. Recent work by Ccallata et al. [8] studied the effect of  $\gamma$ -irradiation and high temperature annealing on the thermoluminescence properties of natural Brazilian green zoisite.

The goal of this study is to explain how absorption bands are produced in the pumpellyite mineral and who are responsible from them, how they varies with both  $\gamma$ -irradiations and heat treatments, just as well to identify the defect responsible for EPR signals. In particular, to understand why heating above 850–900 °C  $Fe^{3+}$  and  $Mn^{2+}$  – signals change. The material is interesting to have a large amount of Mg, which indicates that can be a potential candidate for dosimetry.

In this paper we report a detailed study of OA and EPR spectra of pumpellyite from Rio Grande do Norte–Brazil, rich in Mg. Different temperatures of heat treatment and high doses of gamma radiation were applied to natural samples in order to observe the centers involved in the EPR and OA properties. Crystal Field parameters of pumpellyite were calculated and a model of interaction during the annealed sample was proposed, where  $Mn^{2+}$ ,  $Fe^{2+}$  and  $Fe^{3+}$  ions have a important participation.

## 2. Material and experiments

In this work pumpellyite from the Brejui mine State of Rio Grande do Norte, Brazil, rich in Mg has been investigated concerning to OA and EPR properties. For the OA experiments six slabs with  $1.0 \pm 0.2$  mm thickness were cut and appropriately polished. Enough portion of the pumpellyite sample was crushed and as usual was sieved to retain grains of size between 0.080 and 0.180 mm, smaller grains were used in of X-ray diffraction (XRD) and X-ray fluorescence (XRF) analysis and larger grains were used in EPR measurements.

The chemical composition of our sample was determined by X-ray fluorescence analysis (Phillips PW2404). To certify that the sample to be investigated is actually a pumpellyite X-ray diffraction (XRD) analysis was carried out using MiniFlex II diffractometer. EPR measurements have been carried out in Bruker EMX (X-band) spectrometer with a rectangular cavity ER4025T; the optical spectra were obtained in the Varian Cary Model 500 UV–Vis–NIR spectrometer. All  $\gamma$ -ray irradiations have been done at IPEN–Institute of Energy and Nuclear Research in a  $^{60}Co$  source with a dose rate of  $4.70 \pm 0.09$  kGy $^{-1}$  at room temperature.

## 3. Results and discussion

Table 1 presents in the first column oxides components of the natural pumpellyite used in the present study. For comparison in the second and third columns two synthesized pumpellyite samples components are listed, they are Mg rich and are often cited as examples [9,10]. The last column presents impurity elements in ppm. This result shows relatively large concentration of  $SiO_2$  (47.27%), iron oxide (10.30%),  $TiO_2$  (0.42%) and  $MnO$  (0.365%).

Table 1

X-ray fluorescence analysis of natural pumpellyite. S1: Pumpellyite from Keweenaw Peninsula [9]. S2: Pumpellyite from data base of Duda and Rejl [10].

Oxide (wt%)	Natural	S1	S2	Oxide (ppm)	Natural
CaO	20.90	23.08	23.83	Ba	219
MgO	6.45	3.18	8.56	Cl	307
MnO	0.365	0.13	–	Cr	67
$Al_2O_3$	12.88	23.50	21.66	Cu	348
$SiO_2$	47.27	37.18	38.29	F	5637
$H_2O$	–	6.34	7.65	Pb	57
$Fe_2O_3$	10.30	5.29	–	S	2016
FeO	–	2.09	–	Sr	609
NaO	0.14	0.19	–	Th	63
$K_2O$	0.17	Trace	–	U	3
$TiO_2$	0.42	–	–	V	111
$P_2O_5$	0.13	–	–	Zn	258

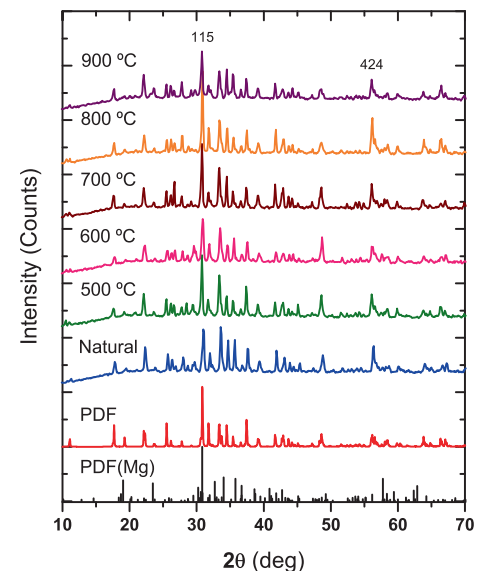
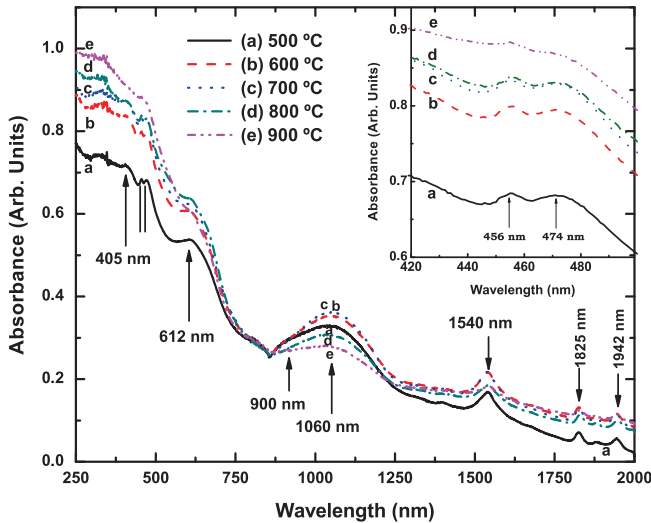


Fig. 1. Diffraction data for natural pumpellyite and samples submitted to high temperature annealing from 500 to 900 °C. Results are compared with two synthesized samples one with basic oxides ones and other one with Mg addition in the structure [11].

X-ray powder diffraction pattern of natural pumpellyite rich in Mg are shown in Fig. 1. The powder patterns are similar to those of other minerals of the epidote group. XRD patterns of pumpellyite without heat treatment and annealed at 500, 600, 700, 800 and 900 °C were compared. Additionally, the intensity of lines and their positions in the diffraction patterns were compared with two synthesized samples of pumpellyite, one with basic components and other with addition of Mg. Note that the most intense diffraction lines belonging to the crystalline phase that characterizes the pumpellyite. Others less intense lines are also found, they are due to impurities with a slight difference in the intensity for one annealing to another. An interesting effect can be seen in lines at 115 and 424, showing to be highest in 800 °C with a subsequent decrease in 900 °C always in the same position. This result confirms that the mineral studied is pumpellyite despite of have being subjected to high temperature annealing.

Fig. 2 shows the optical absorption spectra of natural pumpellyite annealed between 500 and 900 °C. Several bands can be visualized, most of them caused by spin-forbidden transition of  $Fe^{3+}$  and  $Fe^{2+}$  in octahedral sites. As epidote mineral the absorption bands do not change position with thermal treatments, which affect only the intensity of absorption [5]. In particular, bands around 900 and



**Fig. 2.** Optical absorption spectrum of Mg-rich pumpellyite between 250 and 2000 nm. Intense and broad bands are identified such as  $\text{Fe}^{3+}$  and  $\text{Fe}^{2+}$  at octahedral and tetrahedral symmetries.

1060 nm saturate between 700 and 800 °C and beyond this temperature they decrease in intensity. The band around 900 nm is almost hidden by the traced band in 1060 nm after annealing at 900 °C.

Forbidden  $dd$  transitions due the  $\text{Fe}^{3+}$  are shown in Table 2. According to the behavior of the bands in Fig. 2 the broad band around 1060 nm is antisymmetric so we assume that this band is a composition of two types of transitions, a forbidden ( $^6\text{A}_{1g} \rightarrow ^4\text{T}_{1g}$ ) due to  $\text{Fe}^{3+}$  and other allowed ( $^5\text{T}_{2g} \rightarrow ^5\text{E}_g$ ) due to  $\text{Fe}^{2+}$  centered in 900 nm ( $11,111 \text{ cm}^{-1}$ ). On the other hand, bands around 1825 and 1942 nm can be attributed to the  $\text{Fe}^{2+}$  ion in tetrahedral and octahedral symmetries, respectively. Both bands result from strong crystal field in axial direction [12].

From Fig. 2 we can see that from 250 nm to about 600 nm the heights of the bands do not change however there is increase in the background absorption. Particularly the absorption around 612 nm (green) becomes shallow; it disappears after 900 °C annealing, however the absorption between 730 and 900 nm (yellow-red) practically does change with high temperature annealing. In the inset in Fig. 2 the behavior of the bands at 456 and 474 nm is depicted. The height of these band decreases with the annealing temperature. This result has been also observed by Taran et al. [13] and Langer et al. [14], these authors attributed these bands to  $\text{Cr}^{3+}$  ions in octahedral site.

From the wavelengths of several levels transition in  $\text{Fe}^{3+}$  ions in the pumpellyite shown in Table 2, we see that 456 and 474 nm bands are due to  $^6\text{A}_{1g} \rightarrow ^4\text{A}_{1g}, ^4\text{E}_g$  ( $^4\text{G}$ ) transitions, while the broad 1060 nm band is due to  $^6\text{A}_{1g} \rightarrow ^4\text{T}_{1g}$  ( $^4\text{G}$ ) transition, and 612 nm band to  $^6\text{A}_{1g} \rightarrow ^4\text{T}_{2g}$  ( $^4\text{G}$ ) transition. As we can see in Fig. 3 the radiation effect (0.1–3.0 kGy) is very similar to that of high

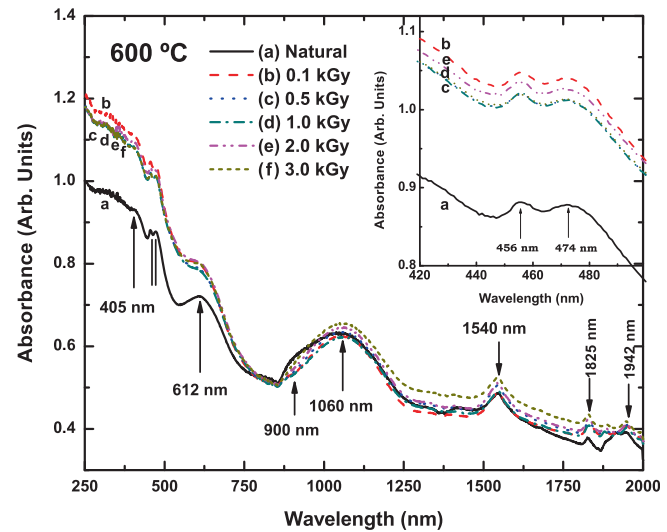


**Fig. 3.** Optical Absorption of pumpellyite pre-annealed in 600 °C them irradiated with 100, 500, 1000, 2000 and 3000 Gy of gamma dose.

temperature annealing for bands between 250 and 900 nm. However, while annealing temperature effect shows increase in 1060 nm band height from 500 °C to around 700 °C and decrease in band height for higher temperature annealing, the  $\gamma$ -radiation dose increased slightly the 1060 nm band saturating around 3 kGy irradiation. In the optical absorption spectrum measurements, we mentioned slightly increases above 700 °C in the broad band around 1060 nm, while 900 nm band decreases slightly, but above this temperature up to 900 °C, 1060 nm band decreases. We assume then that band below 700 °C annealing  $\text{Fe}^{3+}$  is responsible for 900 nm band capture electrons becoming  $\text{Fe}^{2+}$  which increases 1060 nm band due to  $\text{Fe}^{2+}$ . However, by 800–900 °C annealing, now  $\text{Fe}^{2+}$  liberates electrons becoming  $\text{Fe}^{3+}$ . These  $\text{Fe}^{2+}$  ions contribute to dipole–dipole interaction responsible the EPR

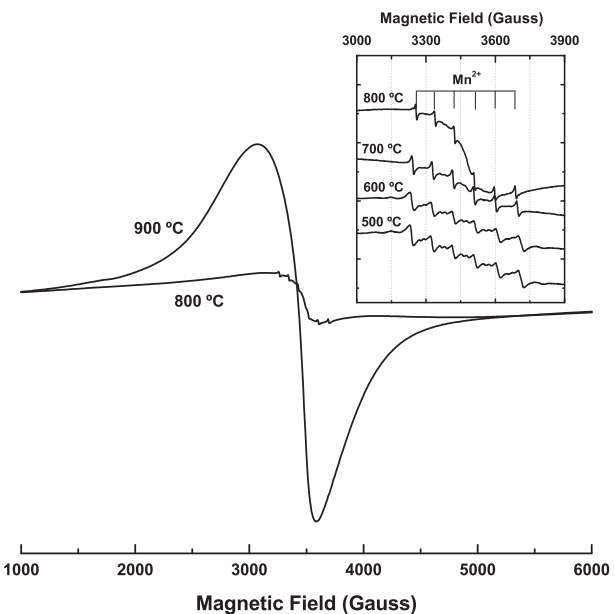


**Fig. 4.** EPR spectrum of pumpellyite. The intense six-line  $\text{Mn}^{2+}$  ( $-1/2 \rightarrow +1/2$ ) transition can be clearly seem near 3300 Gauss. In addition the  $\text{Mn}^{2+}$  inner satellite pair can be clearly identified.

**Table 2**

Energy ( $v$ ) and wavelength ( $\lambda$ ) of spin-forbidden  $dd$  bonds of  $\text{Fe}^{3+}$  ion in spectra of pumpellyite. The positions of bands do not change with increase in annealing temperature.

Transition	$\gamma$ (nm)	$v$ ( $\text{cm}^{-1}$ )
$^6\text{A}_{1g} \rightarrow ^4\text{T}_{1g}$ ( $^4\text{G}$ )	1060	9434
$^6\text{A}_{1g} \rightarrow ^4\text{T}_{2g}$ ( $^4\text{G}$ )	612	16,340
$^6\text{A}_{1g} \rightarrow ^4\text{A}_{1g}, ^4\text{E}_g$ ( $^4\text{G}$ ) {	474	21,097
	456	21,929
$^6\text{A}_{1g} \rightarrow ^4\text{T}_{2g}$ ( $^4\text{D}$ )	405	24,691

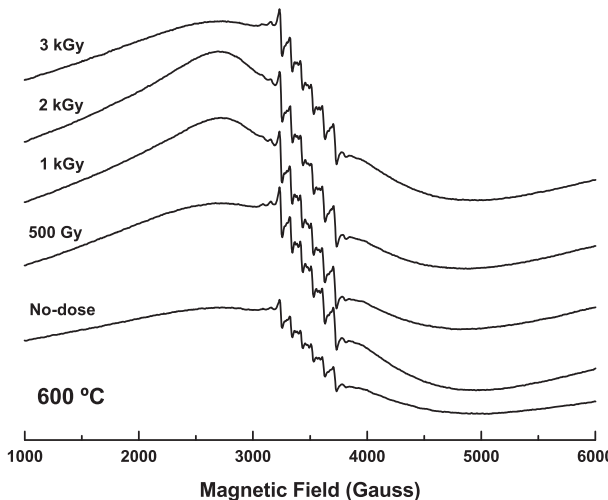


**Fig. 5.** EPR lines of pumpellyite pre-annealed at 600 °C and then irradiated with high radiation gamma dose.

signal around  $g = 2.0$  which becomes as very intense as shown in Fig. 4.

The EPR spectrum of pumpellyite in powder form annealed at from 500 to 900 °C is shown in Fig. 4. The spectrum is characterized by six lines of  $\text{Mn}^{2+}$  centered at  $g = 2.0$  but differing values of  $A$ , i.e., 89.9, 91.8, 93.8, 95.8, 99.7  $\text{cm}^{-1}$  which grow in the direction of magnetic field, see inset in Fig. 4.

A similar study reported by Srinivasulu et al. [4] with zoisite mineral rich in  $\text{Mn}^{2+}$  (Thulite) indicates the same number of lines due to  $\text{Mn}^{2+}$  superimposed on the intense spin–spin interaction due to  $\text{Fe}^{3+}$  ion.

The experimental values of  $g$  and  $A$  are in general agreement with those of  $\text{Mn}^{2+}$  in epidote minerals [3,15]. The hyperfine splitting appears to be independent of orientation of field. Often, the inner satellite pairs ( $\pm 1/2 \rightarrow \pm 3/2$  transitions) are clearly observable; they may be identified from the characteristic hyperfine splitting.

As the temperature annealing increases the shape of six lines  $\text{Mn}^{2+}$ , and their satellites, are slightly distorted. For heat treatment in 800 °C is noted that the signal around  $g = 2.0$  grows significantly and for 900 °C a strong signal of  $\text{Fe}^{3+}$  hidden all  $\text{Mn}^{2+}$  lines. The strong growth of this signal indicates that the transitions due to  $\text{Fe}^{3+}$  dipole–dipole interactions.

Particularly the strong growth of the EPR line at temperatures from 800 to 900 °C can be attributed to the transition  $\text{Fe}^{2+} \rightarrow \text{e}^- + \text{Fe}^{3+}$ . The released electrons can be captured by oxygen vacancies which exists at room temperature but at high temperatures the number increase greatly forming paramagnetic centers, however the EPR signal of these centers is hidden by the huge signal due to  $\text{Fe}^{3+}$ .

The growth of the antisymmetric EPR signal around  $g = 2$  (Fig. 4) indicates that the  $\text{Fe}^{2+}$  and  $\text{Fe}^{3+}$  contribute to this signal. The results

of XRD (Fig. 1) indicate that the crystal structure of pumpellyite resists the severe heat treatment, so that the temperature “critical” 800 °C probably occur a rearrangement of  $\text{Fe}^{2+}$ ,  $\text{Fe}^{3+}$  and  $\text{Mn}^{2+}$  in tetrahedral and octahedral sites of the structure. This rearrangement favors the proximity of iron ions with a strong tendency to form clusters.

Fig. 5 shows the effect of gamma radiation dose on the EPR spectrum of the sample pre-annealed at 600 °C. The  $\text{Mn}^{2+}$  signals do not change, but the radiation up to about 2 kGy increases  $\text{Fe}^{3+}$  signal around  $g = 2$ , at this dose-value EPR signal saturates. This result indicates that high doses of  $\gamma$ -radiation also induce the transition of  $\text{Fe}^{2+} \rightarrow \text{e}^- + \text{Fe}^{3+}$ , but are not strong enough to induce changes as those caused by annealing at high temperature.

#### 4. Conclusions

A sample of pumpellyite, rich in Mg, presented several bands of OA due to allowed and forbidden transitions of  $\text{Fe}^{2+}$  and  $\text{Fe}^{3+}$  in tetrahedral and octahedral environments, respectively.

Samples pre-annealed in high temperature, produced transitions  $\text{Fe}^{2+} \rightarrow \text{e}^- + \text{Fe}^{3+}$ , being more significant for temperatures above 800 °C. An analysis of the EPR spectra showed six lines of  $\text{Mn}^{2+}$  and its satellite pairs  $\pm 1/2 \rightarrow \pm 3/2$  of hyperfine splitting, superimposed on the intense dipole–dipole interaction due to  $\text{Fe}^{3+}$  ion. Only with a heat treatment at 800 °C the signal of  $\text{Mn}^{2+}$  significantly increases but with a heat treatment at 900 °C a strong signal of  $\text{Fe}^{3+}$  hides all lines  $\text{Mn}^{2+}$ . On the other hand high doses of radiation also induce the transition of  $\text{Fe}^{2+}$  to  $\text{Fe}^{3+}$  that increase producing a intense EPR signal around  $g = 2$ .

#### Acknowledgements

We would like to thank Ms. E. Somesari and Mr. C.Gaia for kindly carrying out irradiation of the samples. This work was supported by CAPES and FAPESP.

#### References

- [1] W.A. Deer, J. Zussman, R.A. Howie, *An Introduction to the Rock-Forming Minerals*, second ed., Prentice Hall, 1993.
- [2] W.A. Dollase, *Am. Mineral.* 56 (1971) 447–464.
- [3] T. Tsang, S. Ghose, *J. Chem. Phys.* 54 (1971) 856–862.
- [4] G. Srinivasulu, B.M. Sudhana, B.J. Reddy, R. Natarajan, P.S. Rao, *Spectrochim. Acta A* 48 (1992) 1421–1425.
- [5] M.N. Taran, K. Langer, *Eur. J. Mineral.* 12 (2000) 7–15.
- [6] M. Nagashima, T. Ishida, M. Akasaka, *Phys. Chem. Miner.* 33 (2006) 178–191.
- [7] M. Nagashima, T. Armbruster, E. Libowitzky, *Eur. J. Mineral.* 22 (2010) 333–342.
- [8] H.J. Ccallata, L.T. Filho, S. Watanabe, *Spectrochim. Acta A* 78 (2011) 1272–1277.
- [9] C. Palache, H.E. Vassar, *Am. Mineral.* 10 (1925) 412–418.
- [10] R. Duda, L. Rejl, *Minerals of the World*, Arch Cape Press, New York, 1990.
- [11] A. Yoshiasa, T. Matsumoto, *Am. Mineral.* 70 (1985) 1011–1019.
- [12] G. Hunt, J. Salisbury, *Mod. Geol.* 1 (1970) 283–300.
- [13] M.N. Taran, K. Langer, A.N. Platonov, V. Indutny, *Phys. Chem. Miner.* 21 (1994) 360–372.
- [14] K. Langer, M.N. Taran, A.N. Platonov, *Phys. Chem. Miner.* 24 (1997) 109–114.
- [15] J.W. Robinson (Ed.), *Handbook of Spectroscopy II*, CRC Press, Cleveland, 1974.